

We are IntechOpen, the world's leading publisher of Open Access books Built by scientists, for scientists

6,900

Open access books available

186,000

International authors and editors

200M

Downloads

Our authors are among the

154

Countries delivered to

TOP 1%

most cited scientists

12.2%

Contributors from top 500 universities



WEB OF SCIENCE™

Selection of our books indexed in the Book Citation Index
in Web of Science™ Core Collection (BKCI)

Interested in publishing with us?
Contact book.department@intechopen.com

Numbers displayed above are based on latest data collected.
For more information visit www.intechopen.com



Terminal and Non Terminal Alkynes Partial Hydrogenation Catalyzed by Some d^8 Transition Metal Complexes in Homogeneous and Heterogeneous Systems

Domingo Liprandi, Edgardo Cagnola, Cecilia Lederhos, Juan Badano and Mónica Quiroga

Additional information is available at the end of the chapter

<http://dx.doi.org/10.5772/47742>

1. Introduction

The synthesis and manufacture of food additives, flavours and fragrances, as well as pharmaceutical, agrochemical and petrochemical substances, examples of fine and industrial chemicals, are closely related to selective alkyne hydrogenation [1,2].

Regarding alkyne partial hydrogenation, the main goal is to avoid hydrogenation to single bond and in the case of non-terminal alkynes is to give priority to the highest possible conversion and selectivity to the (Z)-alkene [3-5].

These kind of reactions are carried out by means of a catalytic process where control over conversion and selectivity can be exerted in different ways, e.g.: by varying a) the active species or b) the support, and/or by adding c) a promoter / a poison / a modifier, and finally, and not less important, by modifying the reaction temperature. Examples of factor b) are: mesoporous [6] and siliceous [7] materials, a pumice [8], carbons [9], and hydrotalcite [3]. Cases of factor c) are the typical Lindlar catalyst (palladium heterogenized on calcium carbonate poisoned by lead acetate or lead oxide, Pd-CaCO₃-Pb) [10] and the presence of quinoline and triphenylphosphine [11,12]. Research on factors a) and c) include bi-elemental systems such as Ni-B, Pd-Cu, etc. [13-19]. An example of the effect of the reaction temperature is a paper by Choi and Yoon, who found that the selectivity to (Z)-alkene increases when the temperature decreases using a Ni catalyst [20].

Besides, transition metal complexes are a group of substances widely used as catalysts that could be considered as a new active species or as a metal conditioned by its ligands, a kind of “poison” or a modifier for the metal atom [21].

These coordination compounds, used as catalysts, have gained increasing importance for such reactions [22-28] because they allow getting higher activities and selectivities, even under mild conditions of temperature and pressure [29-33].

The d^8 metals, e.g. Rh(I), Ir(I), Pd(II), Ni(II) and Pt(II), form complexes for which the square planar geometry is specially favoured. They are important in catalysis as the central atom can increase its coordination number by accepting ligands in the apical sites [34] or by interacting with the support. These complexes have also the ability to dissociate molecular dihydrogen, and stabilize a variety of reaction intermediates through coordination as ligands in relatively stable but reactive complexes. This is made possible by promoting rearrangements within their coordination spheres [35].

On the other hand, regarding the physical condition, the desired product can be obtained in homogeneous or heterogeneous systems. The latter, in the context of transition metal complexes used as catalysts, have some practical-economical benefits as follows: a) the easy and cheap way in which the catalyst is removed from the remaining solution after ending the hydrogenation reaction; b) the main product does not need further purification due to a possible contamination with a heavy metal compound when no complex leaching is detected; and lastly, c) there is no need for a costly temperature control.

The purpose of this chapter is to illustrate, based on results already published, the previous ideas using: a) 1-heptyne and 3-hexyne as the substrates to be partially hydrogenated, examples of terminal and non-terminal alkynes respectively, b) $[\text{PdCl}_2(\text{NH}_2(\text{CH}_2)_{12}\text{CH}_3)_2]$ and $[\text{RhCl}(\text{NH}_2(\text{CH}_2)_{12}\text{CH}_3)_3]$ as the catalytic species with coordination spheres having tridecylamine as an electron-donating σ ligand and chloride as an electron-withdrawing σ/π ligand and Pd(II) and Rh(I) as the central atoms respectively and c) $\gamma\text{-Al}_2\text{O}_3$ Ketjen CK 300 and RX3, a commercial carbonaceous material from NORIT, as supports for the heterogeneous catalytic tests.

Last but not least, the complex catalytic performances are compared, at the same operational conditions, against those obtained with the Lindlar catalyst which is accepted as a standard one.

2. Experimental

2.1. Complexes preparation and purification

$[\text{PdCl}_2(\text{TDA})_2]$ and $[\text{RhCl}(\text{TDA})_3]$ (TDA = $\text{NH}_2(\text{CH}_2)_{12}\text{CH}_3$) were prepared in a glass equipment with agitation and reflux in a purified argon atmosphere using tridecylamine (TDA) and PdCl_2 or RhCl_3 according to the case. $[\text{PdCl}_2(\text{TDA})_2]$ (yellow-orange) was obtained at 338 K after 4.0 h with a molar ratio $\text{TDA}/\text{PdCl}_2 = 2$, while $[\text{RhCl}(\text{TDA})_3]$ (yellow) was got at 348 K after 4.5 h with a molar ratio $\text{TDA}/\text{RhCl}_3 = 6$ using toluene and carbon tetrachloride as solvents respectively. The purification was made by column chromatography with silica gel

as the stationary phase using chloroform for $[\text{PdCl}_2(\text{TDA})_2]$ and chloroform/methanol (5/1 vol/vol) for $[\text{RhCl}(\text{TDA})_3]$ as the corresponding eluting solvents. All the aliquots were tested to determine the presence of free TDA by thin layer chromatography. After drying the TDA-free solution in a rotary evaporator each complex, in solid state, was obtained.

2.2. Blank test

In each preceding complex preparation, a blank experiment, using only the corresponding salt and solvent, was run verifying that there was no product obtained from them at all.

2.3. Complexes immobilization

Anchoring of the complexes was carried out on γ -alumina (Ketjen CK 300), previously calcinated in air at 773 K for 3 h, or on RX3 (NORIT), a pelletized commercial carbon, by means of the incipient wetness technique. The solvents used for impregnation were as follows: a) chloroform for $[\text{PdCl}_2(\text{TDA})_2]$ and b) chloroform-methanol 5/1 (vol/vol) for $[\text{RhCl}(\text{TDA})_3]$ using a suitable concentration to obtain 0.3 wt % M (M = Pd or Rh). Then, solvents were let evaporate in a desiccator at 298 K, until constant mass was verified.

In order to check for a possible leaching of the immobilized complexes, each fresh-supported system was subjected to a 100-hour run in the corresponding reaction solvent at 353 K. After the tests, none Pd or Rh metal was detected in the remaining solution by Atomic Absorption spectroscopy, thus revealing a strong complex adherence to each support. In this respect, the constancy of M/Al or M/C atomic ratios obtained by XPS before and after the mentioned tests (see Table 2), ratifies that there was no leaching at all and that the complexes species remained anchored on both supports.

2.4. Complexes characterization

2.4.1. Elemental composition

The presence and weight percent of metal (Pd or Rh), chlorine and nitrogen elements were evaluated for each pure complex on a C- and H-free base, according to standard methods [36-39] to determine the stoichiometric ratios of the main atoms and to give a minimum formula for each complex.

2.4.2. X-Ray photoelectron spectroscopy (XPS)

XPS spectra were carried out to evaluate: a) the electronic state of atoms, b) the atomic ratios, for the pure complexes and for the supported complexes before and after the reaction and (c) the atomic ratios M/Al or M/C (where M = Pd or Rh) for the supported complexes before and after reactions. This was done to get each pure complex minimum formula and some insight in the way the complexes were immobilized on the supports; verifying at the same time that the coordination compounds were maintained after anchoring (fresh catalysts) and after the catalytic evaluations (run catalysts) with the final purpose of demonstrating that the complexes are the real catalytic active species.

A Shimadzu ESCA 750 Electron Spectrometer coupled to a Shimadzu ESCAPAC 760 Data System was used. The C 1s line was taken as an internal standard at 285.0 eV so as to correct possible deviations caused by electric charge on the samples. The superficial electronic states of the atoms were studied according to the position of the following peak maxima: Rh 3d_{5/2} and Pd 3d_{5/2}, N 1s for the TDA molecule and Cl 2p_{3/2} for the complexes in any condition. In order to ensure that there was no modification on the electronic state of the species, the sample introduction was made according to the operational procedure reported elsewhere [40]. Exposing the samples to the atmosphere for different periods of time confirmed that there were no electronic modifications. Determination of the atomic ratios x/Metal (x = N, Cl) and Metal/Z (Z = Al or C, depending on the support) were made by comparing the areas under the peaks after background subtraction and corrections due to differences in escape depths [41] and in photoionization cross sections [42].

2.4.3. Infrared spectroscopy (FTIR and IR)

Pure complexes and TDA IR spectra were taken, in the 4100-900 cm⁻¹ range, to determine the presence of tridecylamine as a ligand in the complexes coordination spheres. The analysis was carried out using the TDA characteristic normal wavenumbers [43-45]. Besides, pure [PdCl₂(TDA)₂] IR spectra was also taken and analyzed, below 600 cm⁻¹, with the purpose to elucidate if the obtained complex was the cis or trans isomer, and consequently to be able to assign a correct local site symmetry for this species.

The high wavenumber spectra were taken in a Shimadzu FTIR 8101/8101M single beam spectrometer; the equipment has a Michelson type optical interferometer. Two chambers are available to improve the quality of the spectra. The first one has a pyroelectric detector made of a high sensitivity LiTaO element, and the other has an MCT detector and the possibility to create a controlled N₂ (or dry air) atmosphere. On the other hand due to the low detector sensitivity below 500 cm⁻¹, a Perkin-Elmer 580 B double beam spectrometer was also used.

All the samples were dried at 353 K and were examined either in potassium bromide or cesium iodide disks in a concentration ranging from 0.5 to 1 wt% to ensure non-saturated spectra [41].

2.4.4. Supports characterization

The porosity of the supports was characterized by physical adsorption of N₂ (77 K) and CO₂ (273 K). Gas adsorption is useful to calculate specific surface area and pore volume. The use of both adsorptives (N₂ and CO₂) allows estimating the pore volume distribution of pores up to about 7.5 nm diameter [46]. By applying the Dubinin-Raduskevich equation to the CO₂ adsorption isotherm at 273 K, the volume of micropores with a diameter less than 0.7 nm (V_{micro}) can be obtained. On the other hand, the volume of supermicropores (V_{supermicro}), diameter ranging from 0.7 to 2 nm, is obtained by subtraction of V_{micro} from the volume calculated by applying the Dubinin-Raduskevich method to the N₂ adsorption isotherm at 77 K [46]. The volume of mesopores with diameter between 2 and 7.5 nm was calculated from the N₂ adsorption isotherm at 77 K. In this respect, the volume of gas adsorbed

between 0.2 and 0.7 relative pressure corresponds to the mesopore range of porosity. The wider porosity, macropores (V_{macro}) and part of the mesopores (with diameter from 7.5 to 50 nm), was determined by mercury porosimetry, using a Carlo Erba 2000 porosimeter. This equipment reaches a maximum pressure of 196 MPa, which allows estimating the volume of pores with a diameter longer than 7.5 nm. The addition of the mesopore volumes determined from N_2 adsorption isotherm and by mercury porosimetry gives the total mesopore volume (V_{meso}) [46]. Finally, with the BET equation applied to the N_2 adsorption isotherm at 77 K it is possible to evaluate the specific surface area.

This information can be used to know the support profitable sites where the complexes can be located and the concentration of the substrates would turn out augmented by a physicochemical adsorption process favouring the partial hydrogenation.

2.4.5. Catalytic runs

The catalytic runs were made using 100 mL of a 2 % v/v alkyne in toluene solution, in a PTFE-coated batch stainless steel stirred tank reactor, operated at 600 rpm during 120 min. The weight of the supported complex catalysts was 0.075 g in all cases. In the catalytic evaluation of the unsupported complexes, a suitable mass of these ones was used to provide the same amount of metal (Pd or Rh) as in the corresponding supported catalysts. The same criterion was used for the Lindlar catalyst. Every catalytic test was carried out in triplicate at $P = 150$ kPa with a relative experimental error of about 3 %.

Detection of possible diffusional limitations during the catalytic runs was taken into account according to the procedures described in the literature [47-48]. External diffusional limitations were examined by varying the stirring velocity in the range of 180-1400 rpm. Conversion and selectivity constancy verified above 500 rpm allows to say that this type of limitation was absent at the selected rotatory speed. On the other hand, intraparticle mass transfer limitations were considered by crushing the heterogenised complex catalyst up to $\frac{1}{4}$ the original size and using the obtained samples to carry out the partial hydrogenation reactions. Conversion and selectivity values, equal to those obtained with the uncrushed heterogenised catalyst, permitted to state that this type of limitation was also absent in the physical operational conditions of our work. Last but not least, the catalyst cylinders were properly treated and weighted after the end of reactions. The difference in the mass of catalyst cylinders (before and after the test reactions) was not appreciable within the experimental error of the analytical balance method, meaning that there was no mass loss from the cylinders. Thus, it can be considered that the attrition effect was absent or was negligible enough to play a role in determining an additional mass transfer limitation. The analysis of reactants and products was made by gas chromatography, using a FID and a CP WAX 52 CB capillary column.

The following substrates and conditions were used to perform the catalytic tests:

- 1-heptyne (a terminal alkyne) partial hydrogenation was used to evaluate the catalytic performance of both complexes in homogeneous condition and anchored on $\gamma\text{-Al}_2\text{O}_3$ at 303 K with a 1-heptyne/Pd or Rh molar ratio equal to $7.3 \cdot 10^3$ and $7.0 \cdot 10^3$, respectively.

- 3-hexyne (a non-terminal alkyne) partial hydrogenation was used to evaluate the catalytic performance of $[\text{RhCl}(\text{TDA})_3]$ in homogeneous condition and anchored on RX3 at 275, 290 and 303 K with a 3-hexyne/Rh molar ratio equal to $8.1 \cdot 10^3$.

2.4.6. Atomic absorption spectroscopy

The possible presence of M (Rh or Pd), provoked by a solvent leaching effect in each solution after catalytic evaluation of the heterogeneous systems, was analyzed by means of the Atomic Absorption technique.

3. Results and discussion

3.1. Pd or Rh complex minimum formula

Table 1 shows M (Pd or Rh), N and Cl elemental composition on a C- and H- free base, as well as Cl/M and N/M molar ratios obtained for the pure complexes.

Complex	Elemental Composition (weight %)			Atomic ratios	
	M	Cl	N	Cl/M	N/M
$[\text{PdCl}_2(\text{TDA})_2]$	52.0	34.3	13.7	1.99	2.00
$[\text{RhCl}(\text{TDA})_3]$	56.9	19.6	23.5	1.00	3.04

Table 1. M (Pd or Rh), N and Cl (on a C- and H-free base) elemental composition and Cl/M and N/M molar ratios for the pure complexes.^[49]

The **Pd:Cl:N** and **Rh:Cl:N** molar ratios for the pure complexes calculated from the weight percent values (Table 1) and the molar masses of these elements, can be expressed as ca. **1:2:2** and **1:1:3** respectively.

Additionally, Table 2 presents the M $3d_{5/2}$, N $1s$ and Cl $2p_{3/2}$ peaks binding energies (BE), and the atomic ratios N/M, Cl/M for the pure and for the fresh and run supported complexes, obtained by XPS.

Table 2 also includes the superficial molar ratio M/Al or M/C for the heterogenized complexes. XPS binding energies for the pure substances are in accordance with the literature values [50,51]; showing that Pd or Rh, N and Cl are present in the corresponding products obtained after the synthesis and purification stages. Besides, the electronic states of these atoms may be considered as follows: a) **$n+$ for Pd or Rh, with $n = 2$ and n close to 1 respectively**; this is based on data in Table 2 and the literature values 338.3 eV for $[\text{PdCl}_2(\text{NH}_3)_2]$ and ranging from 307.3 to 308.5 eV for Rh(I) [50,51]; b) **-3 for N but as an ammonium-like nitrogen** as the $1s$ binding energies in Table 2 fall within the values found in the literature (400.9 to 402 eV [50,51]) corresponding to a NH_4^+ species; **this information suggests a bonding character for the N lone pair towards an electrophilic centre, in this case the Pd or Rh atom**; and c) **-1 for Cl as in a chloride compound** because the $2p_{3/2}$ binding energies in Table 2 are included within the literature values (197.9 to 198.5 eV [50,51]). At the same time, from the mentioned table, the atomic ratios for each complex

indicate that these elements appear in the proportion **Pd:Cl:N equal to 1:2:2 and Rh:Cl:N equal to 1:1:3. These numbers are equal to those obtained via Elemental Composition results.**

Complex	Condition	Binding energies (eV)			Atomic ratios (at/at)		
		M 3d _{5/2}	N 1s	Cl 2p _{3/2}	N/M	Cl/M	M/Al or C
[PdCl ₂ (TDA) ₂]	pure ^[49]	338.2	401.9	198.3	2.00	1.99	-
	γ -Al ₂ O ₃ fresh ^[49]	338.3	401.7	198.2	2.01	2.00	0.09
	γ -Al ₂ O ₃ run ^{a [49]}	338.2	402.0	198.1	1.99	1.99	0.09
	RX3 fresh ^[53]	338.4	401.9	198.2	2.02	2.00	0.10
	RX3 run ^b	338.3	402.0	198.3	2.01	1.99	0.10
[RhCl(TDA) ₃]	pure ^[49]	307.1	402.1	198.1	3.00	1.01	-
	γ -Al ₂ O ₃ fresh ^[49]	307.2	402.2	198.3	2.99	1.02	0.05
	γ -Al ₂ O ₃ run ^{a [49]}	307.1	402.2	198.2	2.99	0.99	0.05
	RX3 fresh ^[52]	307.1	401.9	198.0	3.00	1.02	0.06
	RX3 run ^b	307.0	402.0	198.0	2.99	1.00	0.06

^a 1-heptyne partial hydrogenation

^b 3-hexyne partial hydrogenation

Table 2. XPS binding energies and XPS atomic ratios for pure, fresh and run heterogenized Pd or Rh complexes.

On the other hand, Figure 1 shows the pure TDA, [PdCl₂(TDA)₂] and [RhCl(TDA)₃] FTIR spectra, while Figure 2 depicts the pure [PdCl₂(TDA)₂] IR spectrum in the range below 600 cm⁻¹. As observed at high wavenumbers in Figure 1, the following characteristic peaks of a primary aliphatic amine [44], are present: (A) NH₂ “stretching” (3600-3100 cm⁻¹), CH “stretching” (3000-2800 cm⁻¹), (B) NH₂ “bending” (1700-1600 cm⁻¹), CH “bending” (1500-1300 cm⁻¹) and (C) CN “stretching” (1200-1000 cm⁻¹). In particular, labels A, B and C, related to the nitrogen atom, are taken as a reference because they are sensitive to its environment. Besides Figure 1 shows that [PdCl₂(TDA)₂] and [RhCl(TDA)₃] FTIR peaks globally agree with those corresponding to pure TDA. **Anyhow, differences are found in the labelled wavenumbers indicated above: A, B and C as they show a slight shift to lower frequencies with respect to the pure ligand, meaning an interaction between the nitrogen lone pair and the Pd or Rh atom. This argument is reinforced by the fact that when a primary amine is bonded, the NH₂ stretching peak is considerably different in shape and intensity from the original NH₂ band [45], as seen in the shown spectra. This information confirms that the TDA molecule is one of the ligands in the complexes coordination spheres.**

The IR spectrum presented in Figure 2 shows the peaks corresponding to the Pd-ligand vibrations for the pure complex. **[PdCl₂(TDA)₂] can be considered as the trans-isomer** because of the presence of single peaks, which obey the principle of mutual exclusion, typical of centre-symmetric species [54].

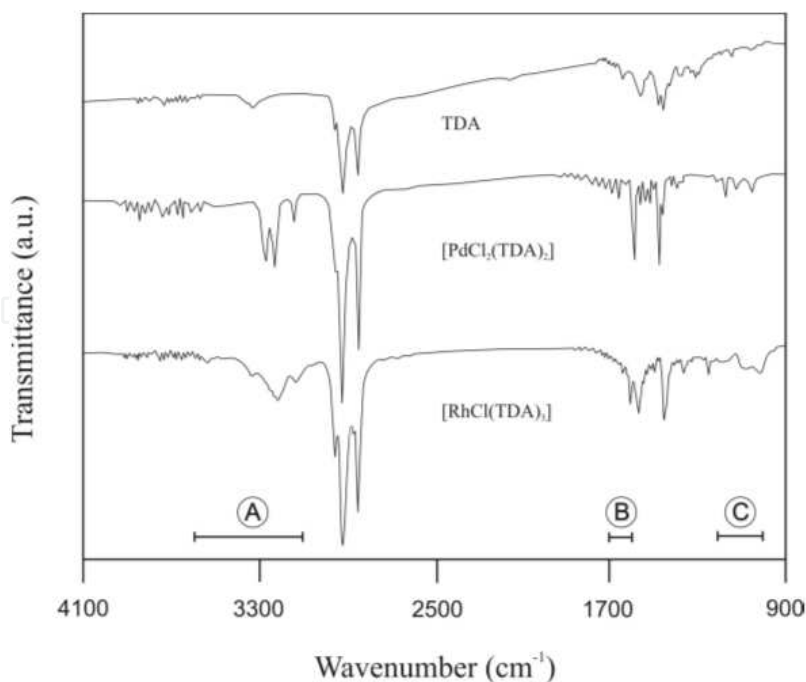


Figure 1. FTIR spectra corresponding to pure TDA, $[\text{PdCl}_2(\text{TDA})_2]$ and $[\text{RhCl}(\text{TDA})_3]$.^[49]

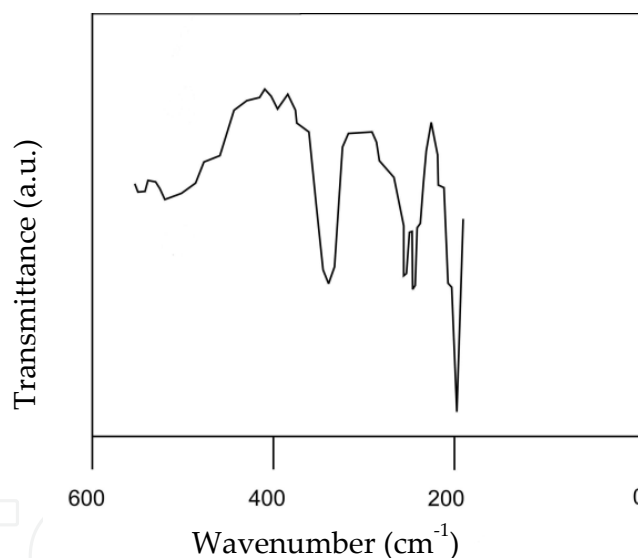


Figure 2. IR spectrum below 600 cm^{-1} for pure $[\text{PdCl}_2(\text{TDA})_2]$.^[54]

At this point, the complex minimum formula, on the basis of the preceding Elemental Composition, XPS and FTIR arguments, can be expressed by $[\text{PdCl}_2(\text{TDA})_2]$ or $[\text{RhCl}(\text{TDA})_3]$.

3.2. Palladium and rhodium local site symmetries, HOMO-LUMO electron configurations and complexes dimensions

Molecular orbitals with symmetries corresponding to the irreducible representations of the molecular point group automatically satisfy the Fock equation. For complex species the terminal atom symmetry orbital (TASO)/molecular orbitals (MO) and the metal atomic

orbitals are taken into account to explain metal-ligand bonding according to their symmetry properties. In this respect, the $(n-1)d$ and ns metal atomic orbitals are those that match best the energy of the TASO/MOs. Based on this, complex antibonding MOs have considerably more metal character while complex bonding MOs have more ligand character; with the former lying higher in energy. On the other hand, tetra-coordinated palladium(II) and rhodium(I) (d^8 species) complexes have a square-planar geometry [55]. On this background and knowing that $[\text{PdCl}_2(\text{TDA})_2]$ is the trans isomer two facts can be considered:

i. HOMO-LUMO Electron Configurations

Knowing that $[\text{PdCl}_2(\text{TDA})_2]$ and $[\text{RhCl}(\text{TDA})_3]$ have a D_{2h} and C_{2v} local site symmetries respectively and taking the main rotation axis along the z cartesian axis, the Angular Overlap Model (AOM) [56] can be used to predict the HOMO-LUMO frontier orbitals in an increasing order of energy for each case:

- $[\text{PdCl}_2(\text{TDA})_2]$
Non-bonding (d_{xy}), antibonding double degenerate $2e^*_\pi$ ($(d_{xz}, d_{yz})^*$), e^*_σ ($(d_{z^2})^*$) and $3e^*_\sigma$ ($(d_{x^2-y^2})^*$) [49]. Assigning the eight electrons to this scheme, it turns out that $(d_{z^2})^*$ (z direction) and $(d_{x^2-y^2})^*$ (x and y directions) are the HOMO and LUMO frontier orbitals, respectively.
- $[\text{RhCl}(\text{TDA})_3]$
Non-bonding (d_{xy}), antibonding double-degenerate e^*_π ($(d_{xz}, d_{yz})^*$), $7/4 e^*_\sigma$ ($(d_{z^2})^*$) and $9/4 e^*_\sigma$ ($(d_{x^2-y^2})^*$). Assigning the eight electrons to this scheme, it turns out that $(d_{z^2})^*$ (z direction) and $(d_{x^2-y^2})^*$ (x and y directions) are the HOMO and LUMO frontier orbitals, respectively.

The Rh(I) complex HOMO-LUMO frontier orbitals lie higher in energy than those corresponding to the Pd(II) complex because of the lower oxidation number of the central atom. The HOMO is useful to produce the cleavage of the H–H bonding, generating hydrogen atoms and the LUMO is available to receive electron density from the substrate molecule, weakening the C–C triple bond; both concepts are key factors during the catalytic cycle leading to the hydrogenation of the substrate.

ii. Complexes Dimensions

The approximate molecular size of the metal complexes can be estimated in order to study structural aspects related to their location in the supports porosity. This can be done taking into account the square planar geometry, typical covalent radii, a 109.5° C–C–C angle and basic trigonometry.

- $[\text{PdCl}_2(\text{TDA})_2]$
The lengths TDA–Pd–TDA and Cl–Pd–Cl are ca. 4 and 0.7 nm, respectively.
- $[\text{RhCl}(\text{TDA})_3]$
The lengths TDA–Rh–TDA and Cl–Rh–TDA are ca. 4 and 2.3 nm, respectively.

3.3. Supported Pd and Rh complexes structures

Table 3 presents the BET surface area and the pore volume distribution for both supports.

Sample	S_{BET} ($\text{m}^2 \text{g}^{-1}$)	V_{micro} (mL g^{-1}) [<0.7 nm]	$V_{\text{supermicro}}$ (mL g^{-1}) [0.7-2 nm]	V_{meso} (mL g^{-1}) [2-7.5 nm]	V_{macro} (mL g^{-1}) [7.5-50 nm]
$\gamma\text{-Al}_2\text{O}_3$	180	0.048	0.030	0.487	0.094
RX3	1411	0.356	0.333	0.098	0.430

Table 3. BET surface area and supports pore volume distributions.^[53]

According to this information it can be remarked that RX3 possesses a S_{BET} that is 7.84 times greater than the $\gamma\text{-Al}_2\text{O}_3$ surface area. Besides, $\gamma\text{-Al}_2\text{O}_3$ can be considered basically a mesoporous support, while RX3 has a pore volume distribution in the range of micro, supermicro and macro pores.

On the other hand, XPS results of binding energies and atomic ratios for the anchored complexes, Table 1, show that: a) Cl/M and N/M atomic ratios are equal to those obtained for the pure complexes and in total accordance with the elemental composition results for the pure complexes; and b) there is a constancy of the M 3d_{5/2}, N 1s and Cl 2p_{3/2} XPS BEs with respect to the corresponding values for the pure complexes, meaning that their electronic states remain unchanged. Item a) indicates that the supported complexes may be considered as tetra-coordinated, maintaining its chemical identity after anchoring, and item b) suggests that the metal (Pd or Rh) is not in contact with the support surface. In this way, as the inductive influence of the hydrocarbon chain on the nitrogen atom is exerted up to the second/third carbon atom, the immobilization of the complexes takes place via a physicochemical interaction between the last part of the TDA molecule and the alumina or carbon basal planes, i.e. an anchoring showing a kind of “table” arrangement as seen in Figure 3.

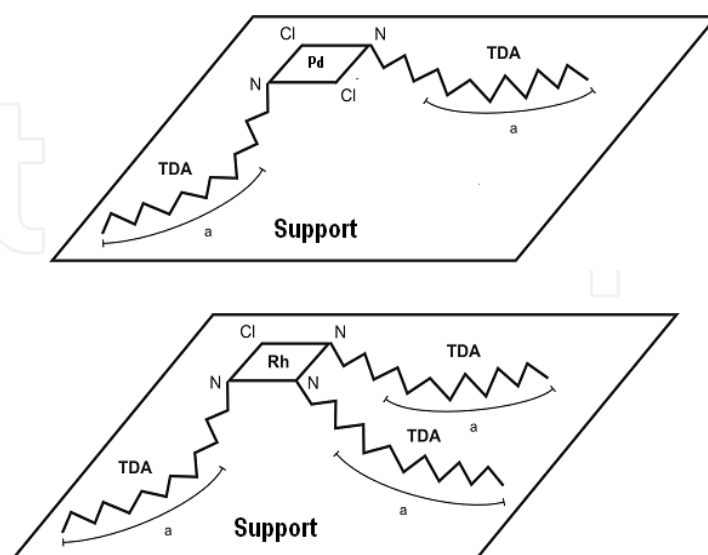


Figure 3. $[\text{PdCl}_2(\text{TDA})_2]$ and $[\text{RhCl}(\text{TDA})_3]$ anchored on $\gamma\text{-Al}_2\text{O}_3$ or RX3, “a” indicates the TDA carbon chain portion involved in the adsorption process.

Based on the ideas of the previous paragraph it can be stated that the anchored complexes maintain the local site symmetries around the central atoms, that is D_{2h} for $[\text{PdCl}_2(\text{TDA})_2]$ and C_{2v} for $[\text{RhCl}(\text{TDA})_3]$, with the same HOMO-LUMO electron configurations.

Besides, as the longest dimension of the coordination compounds is the same for both complexes, and according to the Al_2O_3 or RX_3 distribution pore sizes (Table 3), it can be concluded that the species can be located only in the meso and macropores (2–7.5 and 7.5–50 nm respectively) for both supports, thus occupying ca. 88 % and 43 % of the support total pore volume, respectively.

3.4. Catalytic tests

3.4.1. 1-heptyne partial hydrogenation (terminal alkyne)

1-heptene and n-heptane were the only products detected by GC during the catalytic runs using: (1) commercial Lindlar catalyst, (2) $[\text{PdCl}_2(\text{TDA})_2]$ or $[\text{RhCl}(\text{TDA})_3]$ (homogeneous condition), and (3) $[\text{PdCl}_2(\text{TDA})_2]$ or $[\text{RhCl}(\text{TDA})_3]$ supported on $\gamma\text{-Al}_2\text{O}_3$ (heterogeneous condition) at 303 K, 150 kPa and 2 % v/v 1-heptyne/toluene solution. In Figures 4 and 5, the conversion (X_e) and the selectivity (S_e) to 1-heptene versus 1-heptyne total conversion (X_T) are plotted for all of the catalytic systems.

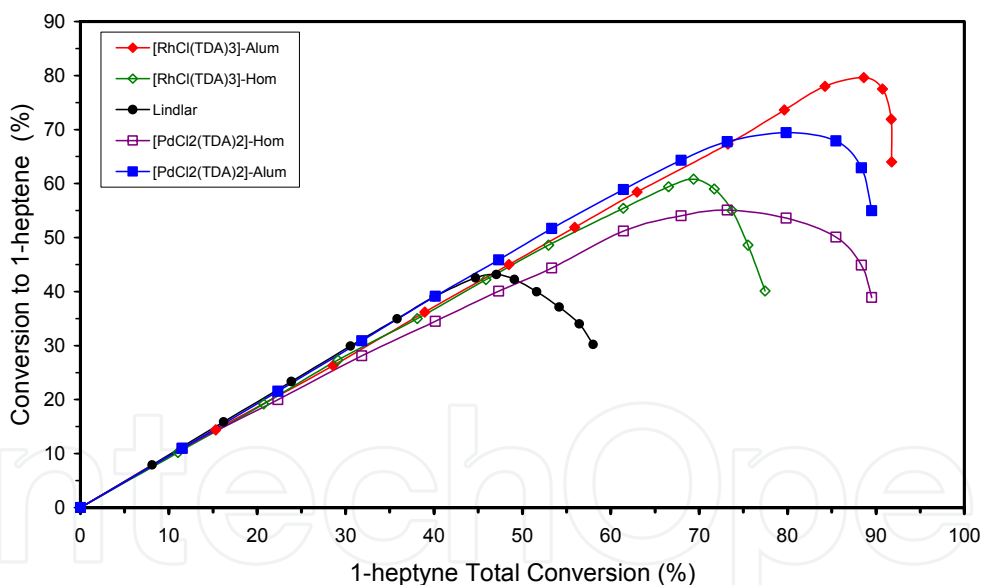


Figure 4. Conversion to 1-heptene vs. 1-heptyne total conversion for: Lindlar catalyst, $[\text{PdCl}_2(\text{TDA})_2]$, $[\text{PdCl}_2(\text{TDA})_2]/\gamma\text{-Al}_2\text{O}_3$, $[\text{RhCl}(\text{TDA})_3]$, $[\text{RhCl}(\text{TDA})_3]/\gamma\text{-Al}_2\text{O}_3$.^[49] 1-heptyne/Pd = $7.3 \cdot 10^3$ and 1-heptyne/Rh = $7.0 \cdot 10^3$.

It can be seen, from Figure 4, that the catalytic systems show an initial part with an almost 45° linear slope. From that part onwards, all the systems show a similar profile shape, with increasing conversion to 1-heptene up to a maximum value, after which this variable falls.

The selectivity plots displayed in Figure 5 show a plateau-shaped behaviour in a very important range of 1-heptyne total conversion followed then by a decreasing tendency.

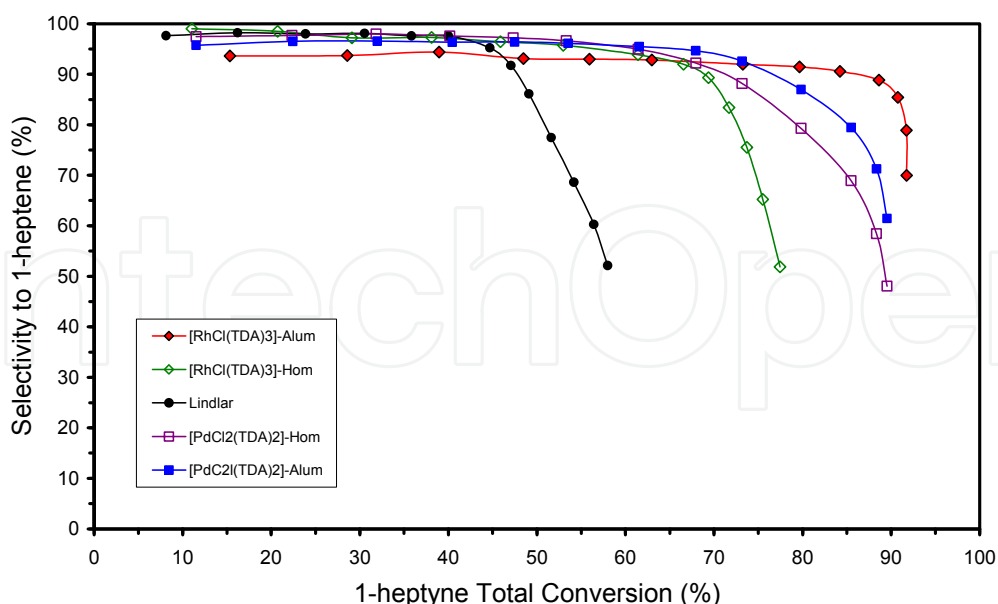


Figure 5. Selectivity to 1-heptene vs. 1-heptyne total conversion for: Lindlar catalyst, $[\text{PdCl}_2(\text{TDA})_2]$, $[\text{PdCl}_2(\text{TDA})_2]/\gamma\text{-Al}_2\text{O}_3$, $[\text{RhCl}(\text{TDA})_3]$, $[\text{RhCl}(\text{TDA})_3]/\gamma\text{-Al}_2\text{O}_3$,^[49] 1-heptyne/Pd = $7.3 \cdot 10^3$ and 1-heptyne/Rh = $7.0 \cdot 10^3$.

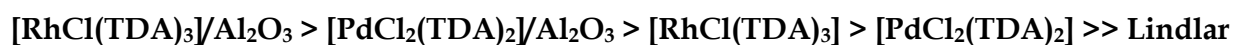
On the other hand, high selectivities to 1-heptene (S_e), which are obtained up to 50 min of reaction time, and their corresponding conversions to 1-heptene (X_e) and 1-heptyne total conversions (X_T), are presented in Table 4.

Catalytic System	Condition	S_e (%)	X_e (%)	X_T (%)
$[\text{RhCl}(\text{TDA})_3]$	Heterogeneous	$\cong 92\text{-}93$	73.6	80.0
	Homogeneous	≥ 92	59.4	66.5
$[\text{PdCl}_2(\text{TDA})_2]$	Heterogeneous	≥ 95	64.3	68.0
	Homogeneous	≥ 92	54.0	67.9
Lindlar	Heterogeneous	≥ 92	43.2	47.1

Table 4. Selectivity and conversion to 1-heptene and 1-heptyne total conversion values for the catalytic systems up to 50 min of reaction. 1-heptyne/Rh = $7.0 \cdot 10^3$ and 1-heptyne/Pd = $7.3 \cdot 10^3$.

With this information, trends and selection of the best catalytic systems are drawn taking into account two factors: a) high selectivity values to 1-heptene and b) the range of 1-heptyne total conversion in which the high selectivity values are maintained.

A general trend, based on the better catalytic performances (Table 4), can be established for the involved systems:



From this trend, it can be stated that $[\text{PdCl}_2(\text{TDA})_2]$ and $[\text{RhCl}(\text{TDA})_3]$ in heterogeneous or homogeneous conditions are better options than the Lindlar catalyst for the 1-heptyne partial hydrogenation under mild operational conditions.

Besides, depending on the central element or the physical condition two new trends can be written:

Central Element: Rh systems are better than Pd systems

Physical Condition: Heterogeneous systems are better than Homogeneous systems

From these tendencies, it can be stated that the best combination is the Rh(I) complex heterogeneous system, which is in the first place in the general trend and the worst option is the Lindlar catalyst.

3.4.2. 3-hexyne Partial Hydrogenation (Non-Terminal Alkyne)

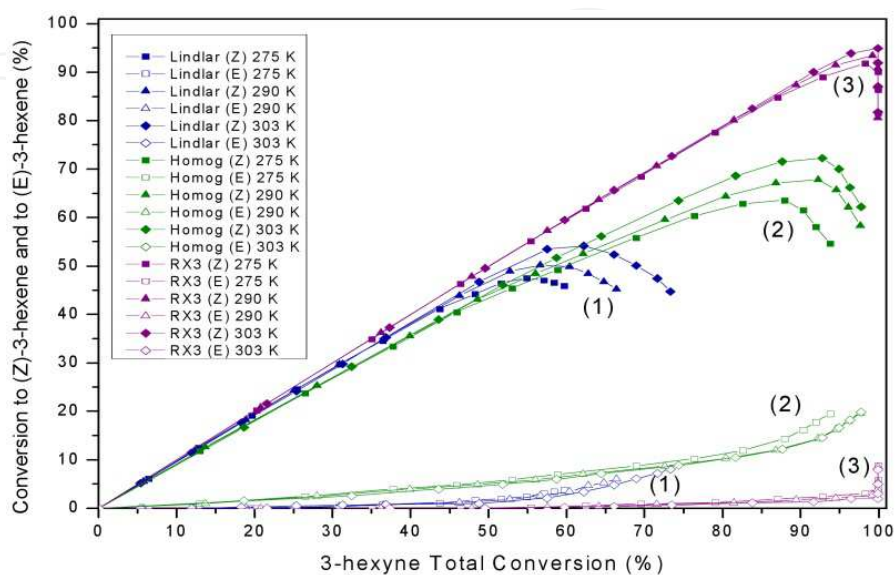
(*Z*)-3-hexene, (*E*)-3-hexene and n-hexane were the only products detected by GC during the reaction tests using the catalytic systems: (1) commercial Lindlar catalyst (2) $[\text{RhCl}(\text{TDA})_3]$ (homogeneous condition), and (3) $[\text{RhCl}(\text{TDA})_3]/\text{RX3}$ (heterogeneous condition) at 275, 290 and 303 K, 150 kPa and 2 % v/v 3-hexyne/toluene solution. In Figure 6(a) the conversions to (*Z*)-3-hexene and (*E*)-3-hexene are shown as a function of the 3-hexyne total conversion for the Lindlar catalyst and for Rh(I) homogeneous and heterogeneous complex for the three temperatures, while Figure 6(b), for the sake of clarity, is presented at the optimum temperature 303 K. It can be noted the predominant formation of the (*Z*)-alkene stereoisomer, the desired product. In this respect, it can be seen in Figure 6, that all of the catalytic systems show again an initial part with an almost linear slope, which takes a value of 45° for the $[\text{RhCl}(\text{TDA})_3]/\text{RX3}$ catalyst. After that initial part, all of the systems have a similar shape with an increasing 3-hexyne total conversion, showing a maximum value of conversion to (*Z*)-3-hexene. There was also a relatively low amount of the side products: (*E*)-3-hexene formed either as initial product or via $Z \rightarrow E$ isomerization, and n-hexane (not plotted in Figure 6 because of the low values obtained and for the sake of clarity) produced either by hydrogenation of the alkyne or the alkene isomers [7,57]. Last but not least, $[\text{RhCl}(\text{TDA})_3]/\text{RX3}$ showed the lowest conversion values to the (*E*) isomer and to the alkane.

In Figure 7, a detail from Figure 6, it can be observed that, for a given catalytic system, the variation of conversion to (*Z*)-3-hexene vs. 3-hexyne total conversion follows an increasing tendency as the temperature is raised. However, it can be noted that the performance of Rh(I) complex heterogeneous system is slightly sensitive to temperature changes while the homogeneous system and the Lindlar catalyst are considerably sensitive to temperature changes.

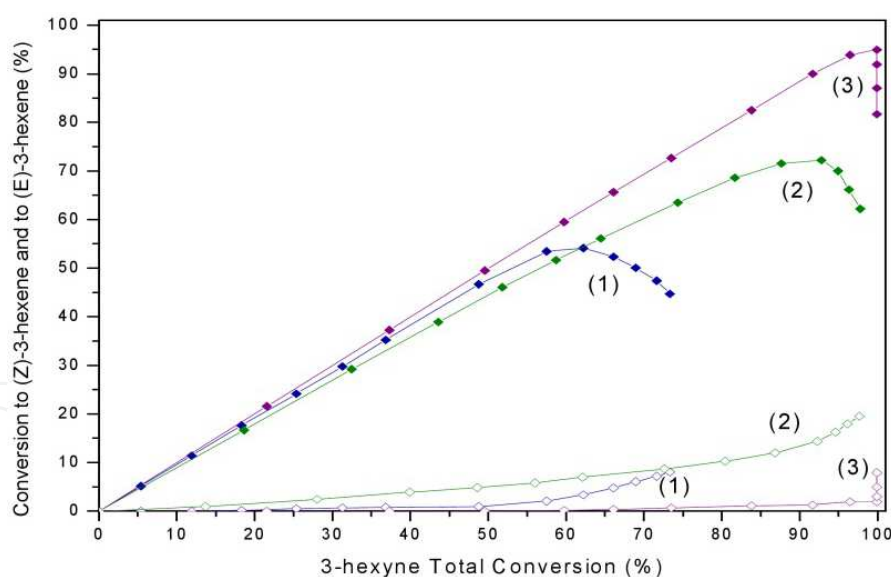
For a given temperature, the $[\text{RhCl}(\text{TDA})_3]/\text{RX3}$ system shows the highest conversions to (*Z*)-3-hexene at the highest 3-hexyne total conversions (maximum value: $X_{(Z)} = 95.0\%$ at $X_T = 99.8\%$), followed by $[\text{RhCl}(\text{TDA})_3]$ and then by the Lindlar catalyst.

In Figure 8 the selectivity to (*Z*)-3-hexene vs. the 3-hexyne total conversion values are presented. The selectivity plots show an initial plateau-shaped behaviour followed by a marked decreasing tendency for the increasing 3-hexyne total conversion. The $[\text{RhCl}(\text{TDA})_3]/\text{RX3}$ system allows to obtain a practically constant value of a very high selectivity (not lower than 98.5%) up to a very high 3-hexyne total conversion (ca. 85%); after

that, the selectivity decays to a value ca. 82 %. Meanwhile, in the case of $[\text{RhCl}(\text{TDA})_3]$ and the Lindlar catalyst, high values of selectivities (ca. 89.4 and ca. 94.2 respectively) were obtained for lower 3-hexyne total conversions up to ca. 44%; then both systems show a monotonously decreasing profile shape, which is more pronounced in the case of the Lindlar catalyst.



(a)



(b)

Figure 6. (a) Conversion to (*Z*)-3-hexene and to (*E*)-3-hexene vs. 3-hexyne total conversion for: (1) Lindlar catalyst, (2) $[\text{RhCl}(\text{TDA})_3]$, (3) $[\text{RhCl}(\text{TDA})_3]/\text{RX3}$; filled square/open square 275 K, filled triangle/open triangle 290 K, filled diamond/open diamond 303 K. Open symbols: (*E*)-3-hexene, solid symbols (*Z*)-3-hexene.^[54] 3-hexyne/Rh = $8.1 \cdot 10^3$.

(b) Conversion to (*Z*)-3-hexene and to (*E*)-3-hexene vs. 3-hexyne total conversion for: (1) Lindlar catalyst, (2) $[\text{RhCl}(\text{TDA})_3]$, (3) $[\text{RhCl}(\text{TDA})_3]/\text{RX3}$; at the optimum temperature 303 K. Open symbols: (*E*)-3-hexene, solid symbols (*Z*)-3-hexene.^[54] 3-hexyne/Rh = $8.1 \cdot 10^3$.

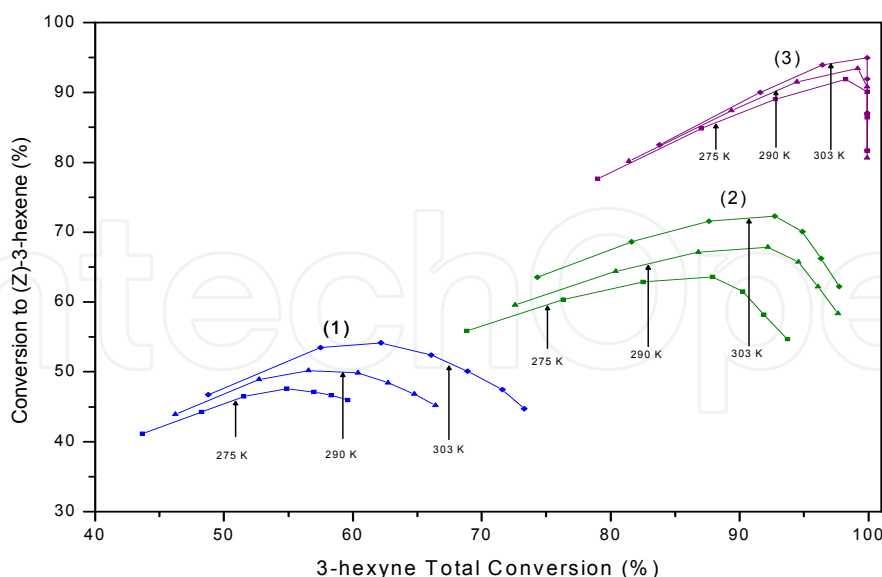


Figure 7. Conversion to (Z)-3-hexene vs. 3-hexyne total conversion for: (1) Lindlar catalyst, (2) $[\text{RhCl}(\text{TDA})_3]$, (3) $[\text{RhCl}(\text{TDA})_3]/\text{RX3}$ (a detail of Figure 6 in the zone where the three systems present the most remarkable differences).^[54] 3-hexyne/Rh = $8.1 \cdot 10^3$.

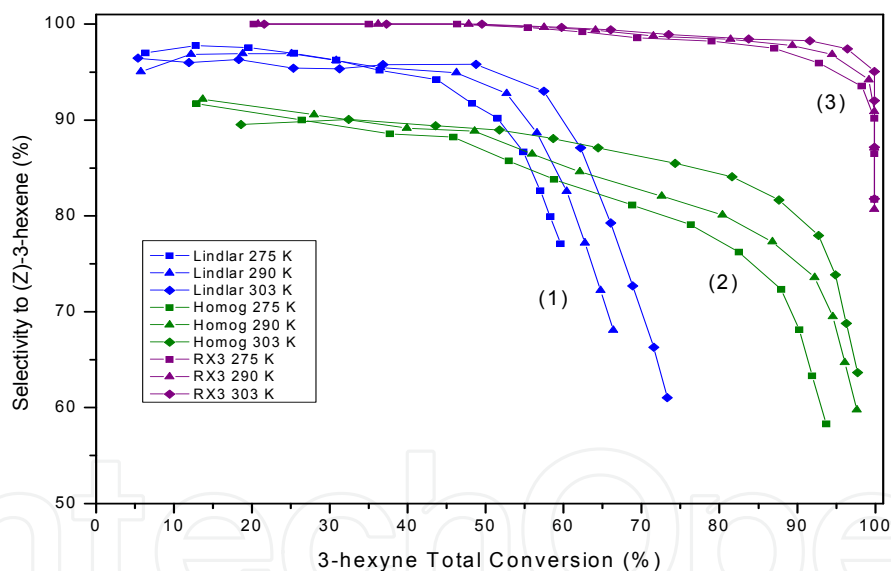


Figure 8. Selectivity to (Z)-3-hexene vs. 3-hexyne total conversion for: (1) Lindlar, (2) $[\text{RhCl}(\text{TDA})_3]$, (3) $[\text{RhCl}(\text{TDA})_3]/\text{RX3}$; (●) 275 K, (▲) 290 K, (◆) 303 K.^[54] 3-hexyne/Rh = $8.1 \cdot 10^3$.

To reinforce the conclusions given in the previous paragraphs, some relevant conversion and selectivity values for diverse reaction conditions are summarized in Table 5.

Considering Figures 6, 7 and 8 and Table 5 the different catalytic systems can be ordered in a descendent $X_{(Z)}$ production as follows: $[\text{RhCl}(\text{TDA})_3]/\text{RX3} > [\text{RhCl}(\text{TDA})_3] \gg$ Lindlar catalyst. Finally, for each system the higher the temperature the higher the selectivity and the higher the conversion to the (Z)- isomer, although the $[\text{RhCl}(\text{TDA})_3]/\text{RX3}$ system behaves as the less sensitive catalyst to that variable.

Reaction time (min)	Catalyst	T (K)	X _T (%)	X _(Z) (%)	S _(Z) (%)	S _(E) (%)	S _n (%)
50	Lindlar	275	48	44	92	3	5
		290	53	49	93	3	4
		303	57	53	93	4	3
	[RhCl(TDA) ₃]	275	76	61	79	13	8
		290	81	64	80	13	7
		303	82	69	84	13	3
	[RhCl(TDA) ₃]/RX3	275	87	85	98	2	0.3
		290	89	87	98	2	0.3
		303	92	90	98	1.5	0.5
120	Lindlar	275	60	46	77	6	17
		290	66	45	68	9	23
		303	73	44	61	11	28
	[RhCl(TDA) ₃]	275	94	55	58	21	21
		290	98	58	59	20	21
		303	98	62	64	20	16
	[RhCl(TDA) ₃]/RX3	275	99.9	82	82	9	9
		290	99.9	81	81	8	11
		303	99.9	82	82	8	10

Table 5. 3-hexyne total conversion (X_T), conversions to (Z)-3-hexene (X_(Z)) and selectivities to (Z)-3-hexene (S_(Z)), (E)-3-hexene (S_(E)) and n-hexane (S_n) for the following catalysts: Lindlar, [RhCl(TDA)₃] complex unsupported and anchored on RX3. 3-hexyne/Rh = 8.1 10³.

It can be remarked that for the 3-hexyne (non-terminal alkyne) partial hydrogenation, [RhCl(TDA)₃] is a much better option than the Lindlar catalyst to obtain the desired product.

3.5. The optimum catalytic system for both test reactions

3.5.1. Chemical considerations

Based on the information obtained from the previous sections, it can be concluded that [RhCl(TDA)₃], supported either on γ -Al₂O₃ or on RX3 in a “table” arrangement structure (Section 3.3), is the best option to carry out the 1-heptyne or 3-hexyne partial hydrogenation to obtain high conversion values. As it was said in Section 3.2, this complex has a d⁸ central element with a combination of ligands L'/L = 3 (L' = TDA, L = Cl), with a square planar geometry associated to a C_{2v} local site symmetry. This type of coordination compound, at some point of the reaction mechanism, has to release one of the coordination sphere ligands; in this respect, the trans-effect series indicates that the labile ligand is TDA opposite to the Cl ligand. Some features related to the central atom, the TDA ligand, the complex coordination number, the site symmetry and the supported condition, could explain this optimum performance.

According to the Atomic Orbital Model (AOM) mentioned in Section 3.2, the $(d_{z^2})^*$ and $(d_{x^2-y^2})^*$ are the HOMO/LUMO frontier orbitals, respectively. The former, along the z axis with a high electron density, is ready to overlap with the hydrogen σ antibonding orbital, thus favouring H-H bond breaking and the latter, an empty orbital extended on the xy plane, is available to receive electron density from the substrate molecule triple bond, thus weakening its π bonds. These two factors, that are important in the hydrogenation catalytic cycle, will be particularly favoured in this case as the complex antibonding orbitals have considerably more metal than ligand character with a relatively high energy because of the low oxidation state of the central element.

On the other hand, the complex bonding molecular orbitals have a predominant character from the TAO/MOs of the ligands in the coordination sphere constituted by tridecylamine (an electron donating σ species) and chloride (an electron-withdrawing σ/π species) in a 3/1 ratio what means a net electronic enrichment on the Rh atom, a fact that will also contribute to the H-H bond rupture. Besides, the TDA ligand presents another remarkable feature related to the Dispersion forces which are relevant when the TDA/solvent interaction is analyzed. This is important as soon as the TDA molecule is released, due to the trans-effect, and it is simultaneously stabilized by the solvent via a solvation process, a fact that is greatly favoured because of the long hydrocarbon chain of the TDA ligand.

Besides, the presence of a support, either $\gamma\text{-Al}_2\text{O}_3$ or RX_3 , can favour the catalytic process by activating some extra substrate molecules (1-heptyne or 3-hexyne) because of their interactions with the support surface via Acid/Base Lewis or Dispersion forces for $\gamma\text{-Al}_2\text{O}_3$ or RX_3 respectively. In any case, this situation turns out to be an important factor as it makes the alkyne (1-heptyne or 3-hexyne) concentration around the supported complex higher than in the bulk solution.

Finally, the high selectivity values could be explained considering the interaction between the substrate triple or double bond (alkyne or alkene) with the complex species LUMO frontier orbital, and, additionally, for the heterogeneous system, with the support chemical sites. For both factors the stronger the interaction, the more favourable the hydrogenation process, but in each case a triple bond will give place to the strongest interaction. Thus, the selectivity to 1-heptene or (*Z*)-3-hexene will be kept in a very high value inasmuch as the alkyne concentration is high enough to consider the alkene hydrogenation negligible, after that the situation is reversed.

3.5.2. Practical considerations

On the other hand, regarding that $[\text{RhCl}(\text{NH}_2(\text{CH}_2)_{12}\text{CH}_3)_3]$ anchored on $\gamma\text{-Al}_2\text{O}_3$ or RX_3 is the optimum catalyst, some practical-economical benefits can be mentioned: a) the easy and cheap way in which the catalyst is removed from the remaining solution after ending the hydrogenation reaction; b) the main product does not need further purification due to a possible contamination with a heavy metal compound as no complex leaching was detected; and lastly, c) there is no need for a costly temperature control due to the mild operational conditions.

4. Conclusions

Experimental results demonstrate that $[\text{PdCl}_2(\text{NH}_2(\text{CH}_2)_{12}\text{CH}_3)_2]$ and $[\text{RhCl}(\text{NH}_2(\text{CH}_2)_{12}\text{CH}_3)_3]$, d^8 transition metal complexes, can be used as catalysts to partially hydrogenate 1-heptyne and 3-hexyne (terminal and non-terminal alkynes respectively) in homogeneous and heterogeneous systems ($\gamma\text{-Al}_2\text{O}_3$ and RX_3 as supports) at mild operational conditions ($P = 150$ kPa and T up to 303K) with very good catalytic performances even better than the Lindlar catalyst. Analyses based on Elemental Composition, XPS, IR, Atomic Absorption Spectroscopy show that the active catalytic species is the complex itself in each case, with a minimum formula as written above.

Tetracoordinated electron-rich transition elements, as well as the presence and the relative quantity of a good electron donating ligand such as $\text{NH}_2(\text{CH}_2)_{12}\text{CH}_3$ with a long-chain hydrocarbon substituent and the heterogeneous condition, contribute to obtain a catalytic system with a high activity and selectivity performance. According to this and supported by experimental results, the optimum catalyst turns out to be $[\text{RhCl}(\text{NH}_2(\text{CH}_2)_{12}\text{CH}_3)_3]$ supported either on $\gamma\text{-Al}_2\text{O}_3$ or RX_3 . This behaviour can be understood in terms of Coordination Sphere parameters, Complex Dimensions, Local Site Symmetry, HOMO/LUMO frontier orbitals and some Support features

Author details

Domingo Liprandi^{1*}, Edgardo Cagnola¹, Cecilia Lederhos²,
Juan Badano² and Mónica Quiroga^{1,2}

¹*Inorganic Chemistry, Department of Chemistry, Faculty of Chemical Engineering, National University of Litoral (UNL), Santa Fe, Argentina,*

²*Institute of Catalysis and Petrochemistry Research, INCAPE (CONICET- UNL), Santa Fe, Argentina*

Acknowledgement

UNL and CONICET financial supports are greatly acknowledged.

5. References

- [1] Chen B, Dingerdissen U, Krauter JGE, Lansink Rotgerink HGJ, Móbus K, Ostgard DJ, Panste P, Riermeir TH, Seebald S, Tacke T, Trauthwein H (2005) New developments in hydrogenation catalysis particularly in synthesis of fine and intermediate chemicals. *App.Catal. A: Gen.* 280:17-46.
- [2] Elsevier CJ, Kluwer AM (2007) Homogeneous hydrogenation of alkynes and dienes. In: de Vries JG, Elsevier CJ (eds) *Handbook of homogeneous hydrogenation*. vol 1, ch 14. Wiley-VCH, Darmstadt, p 375

* Corresponding Author

- [3] Mastalir A, Király Z (2003) Pd nanoparticles in hydrotalcite: mild and highly selective catalysts for alkyne semihydrogenation. *J. Catal.* 220: 372-381.
- [4] Marín-Astorga N, Pecchi G, Fierro JLG, Reyes P (2003) Alkynes hydrogenation over Pd-supported catalysts. *Catal. Lett.* 91 (1–2):115-121.
- [5] Semagina N, Kiwi-Minsker L (2009) Palladium Nanohexagons and Nanospheres in Selective Alkyne Hydrogenation. *Catal. Lett.* 127 (3–4):334-338.
- [6] Choudary BM, Kantam ML, Reddy NM, Rao KK, Haritha Y, Bhaskar V, Figueras F, Tuel A (1999) Hydrogenation of acetylenics by Pd-exchanged mesoporous materials. *App. Catal. A; Gen.* 181:139-144.
- [7] Li F, Yi X, Fang W (2009) Effect of Organic Nickel Precursor on the Reduction Performance and Hydrogenation Activity of Ni/Al₂O₃ Catalysts. *Catal. Lett.* 130:335-340.
- [8] Gruttadauria M, Noto R, Deganello G, Liotta LF (1999) Efficient semihydrogenation of the C-C triple bond using palladium on pumice as catalyst. *Tetrahedron Lett.* 40:2857-2858.
- [9] Lennon D, Marshall R, Webb G, Jackson SD (2000) The effects of hydrogen concentration on propyne hydrogenation over a carbon supported palladium catalyst studied under continuous flow conditions. *Stud. Surf. Sci. Catal.* 130: 245-250.
- [10] Lindlar H, Dubuis R, Jones FN, McKusick FC (1973) Palladium catalyst for partial reduction of acetylenes. *Org. Synth. Coll.* 5: 880.
- [11] Yu J, Spencer JB (1998) Discovery that quinoline and triphenylphosphine alter the electronic properties of hydrogenation catalysts. *Chem. Comm.* 1103-1104
- [12] Nijhuis TA, van Koten G, Kapteijn F, Moulijn JA (2003) Separation of kinetics and mass-transport effects for a fast reaction: the selective hydrogenation of functionalized alkynes. *Catal. Today* 79–80: 315-321.
- [13] Huang W, Li A, Lobo RF, Chen JG (2009) Effects of Zeolite Structures, Exchanged Cations, and Bimetallic Formulations on the Selective Hydrogenation of Acetylene Over Zeolite-Supported Catalysts. *Catal. Lett.* 130: 380-385.
- [14] Badano JM, Quiroga M, Betti C, Vera C, Canavese S, Coloma-Pascual F (2010) Resistance To Sulfur And Oxygenated Compounds Of Supported Pd, Pt, Rh, Ru Catalysts. *Catal. Lett.* 137: 35-44.
- [15] Nijhuis TA, van Koten G, Moulijn JA (2003) Optimized palladium catalyst systems for selective liquid-phase hydrogenation of functionalized alkynes. *App. Catal. A: Gen.* 238: 259-271.
- [16] Chen JG, Qi S-T, Humbert MP, Menning CA, Zhu Y-X (2010) Rational design of low-temperature hydrogenation catalysts: Theoretical predictions and experimental verification. *Acta Phys. Chim. Sin.* 26 (4): 869-876.
- [17] Shiju RN, Gulians VV (2009) Recent developments in catalysis using nanostructured materials. *Appl. Catal. A: Gen.* 356: 1-17.
- [18] Volpe MA, Rodríguez P, Gigola CE (1999) Preparation of Pd/Pb/ α -Al₂O₃ catalysts for selective hydrogenation using PbBu₄: the role of metal-support boundary atoms and the formation of a stable surface complex. *Catal. Lett.* 61: 27-32

- [19] Zhang W, Li L, Du Y, Wang X, Yang P (2009) Gold/Platinum Bimetallic Core/Shell Nanoparticles Stabilized by a Fréchet-Type Dendrimer: Preparation and Catalytic Hydrogenations of Phenylaldehydes and Nitrobenzenes. *Catal. Lett.* 127 (3–4): 429-436.
- [20] Choi J, Yoon NM (1996) An excellent nickel boride catalyst for the cis-selective semihydrogenation of acetylenes. *Tetrahedron Lett.* 37 (7): 1057-1060.
- [21] Crespo-Quesada M, Dykeman RR, Laurenczy G, Dyson PJ, Kiwi-Minsker L (2011) Supported nitrogen-modified Pd nanoparticles for the selective hydrogenation of 1-hexyne. *J. Catal.* 279: 66-74.
- [22] Costa M, Pelagatti P, Pelizzi C, Rogolino D (2002) Catalytic activity of palladium(II) complexes with tridentate nitrogen ligands in the hydrogenation of alkenes and alkynes. *J. Molec. Catal. A: Chem.* 178: 21-26.
- [23] de Wolf E, Spek AL, Kuipers BWM, Philipse AP, Meeldijk JD, Bomans PHH, Frederik P.M., Deelman B.J., van Koten G. (2002) "Fluorous derivatives of [Ru(COD)(dpppe)]BX₄ (X=F, Ph): synthesis, physical studies and application in catalytic hydrogenation of 1-alkenes and 4-alkynes. *Tetrahedron* 58: 3911-3922.
- [24] Edvrard D, Groison K, Mugnier Y, Harvey PD (2004) The Pd₄(dppm)₄(H)₂²⁺ cluster: a precatalyst for the homogeneous hydrogenation of alkynes. *Inorg. Chem.* 43: 790-796.
- [25] Frediani P, Giannelli C, Salvini A, Ianelli S (2003) Ruthenium complexes with 1,1'-biisoquinoline as ligands. Synthesis and hydrogenation activity. *J. Organomet. Chem.* 667: 197-208.
- [26] Kerr JM, Suckling CJ (1988) Selective hydrogenation by novel palladium(II) complex. *Tetrahedron Lett.* 29 (43): 5545-5548.
- [27] Park JW, Chung YM, Suh YW, Rhee HK (2004) Partial hydrogenation of 1,3-cyclooctadiene catalyzed by palladium-complex catalysts immobilized on silica. *Catal. Tod.* 93-95: 445-450.
- [28] Santra PK, Sagar P (2003) Dihydrogen reduction of nitroaromatics, alkenes, alkynes using Pd(II) complexes both in normal and high pressure conditions. *J. Molec. Catal. A: Chem.* 197 (1-2): 37-50.
- [29] L'Argentièrè PC, Cagnola EA, Cañón MG, Liprandi DA, Marconetti DV (1998), A nickel tetra-coordinated complex as catalyst in heterogeneous hydrogenation. *J. Chem. Technol. Biotechnol.* 71: 285-290.
- [30] Quiroga ME, Cagnola EA, Liprandi DA, L'Argentièrè PC (1999) Supported Wilkinson's complex used as a high active hydrogenation catalyst. *J. Mol. Catal. A: Chem.* 149: 147-152.
- [31] Liprandi DA, Quiroga ME, Cagnola EA, L'Argentièrè PC (2002) A new more sulfur-resistant rhodium complex as an alternative to the traditional Wilkinson's catalyst. *Ind. Eng. Chem. Res.* 41: 4906-4910
- [32] Cagnola EA, Quiroga ME, Liprandi DA, L'Argentièrè PC (2004) Immobilized Rh, Ru, Pd and Ni complexes as catalysts in the hydrogenation of cyclohexene. *Appl. Catal. A: Gen.* 274: 205-212.
- [33] Hamilton CA, Jackson SD, Kelly GJ, Spence R, Bruin D (2002) Competitive Reactions in Alkyne Hydrogenation. *App. Catal. A: Gen.* 237: 201-209.
- [34] Bailar J C, (ed) (1975) *Comprehensive Inorganic Chemistry*. Vol 3, p. 1234.

- [35] Halpern J (1968) in: *Homogeneous Catalysis*. American Chemical Society: Chap. 1.
- [36] Kolthoff IM, Sandell EB, Meehan EJ, Bruckenstein S (1969) *Quantitative Chemical Analysis*, fourth ed., Interscience Publishers, New York.
- [37] Anderson SN, Basolo F (1963) *Inorg. Synth.* 7: 214-220.
- [38] Vogel AI (1951) *A Text Book of Quantitative Inorganic Analysis*, Longmans, Green and Co, London.
- [39] Livingstone S, in: Bailar JC Jr, Emeléus H., Nyholm R, Trotman-Dickenson AF (Eds.) (1973) *The Chemistry of Ruthenium, Rhodium, Palladium, Osmium, Iridium and Platinum*, *Comprehensive Inorganic Chemistry*, Pergamon Press, Oxford.
- [40] Mallat T, Petrov J, Szabó S, Sztatisz J (1985) Palladium-cobalt catalyst: phase structure and activity in liquid phase hydrogenations. *Reac. Kinet. Catal. Lett.* 29: 353-361.
- [41] Borade R, Sayari A, Adnot A, Kaliaguine S (1990) *J. Phys. Chem.* 94: 5989.
- [42] Scofield JH (1976) *J. Electron. Spectrosc. Relat. Phenom.* 8: 129.
- [43] Nakamoto K (1986) *Infrared and Raman Spectra of Inorganic and Coordination Compounds*, 4th Ed., Wiley, New York, parts I and III.
- [44] Silverstein RM, Clayton Basler G, Morrill TC, *Spectrometric Identification of Organic Compounds*, 5th Ed. Wiley, New York, 1991, chapter III.
- [45] Pouchert CJ (1981) *The Aldrich Library of Infrared Spectra Ed. (III)*: 1562 D.
- [46] Rodríguez-Reinoso F, Linares-Solano A (1988) in: *Chemistry and Physics of Carbon*, Vol. 21, Walker PL Jr. (Ed) ,Marcel Dekker, New York p1.
- [47] Holland FA, Chapman FS (1976) *Liquid Mixing and Processing in Stirred Tanks*, Reinhold, New York, Chap 5.
- [48] Le Page JF (1978) *Catalyse de Contact*, Editions Technip, Paris, Chap 2.
- [49] Quiroga M, Liprandi D, Cagnola E, L'Argentièrre P (2007) 1-heptyne semihydrogenation catalyzed by palladium or rhodium complexes. Influence of: metal atom, ligands and the homo/heterogeneous condition. *Appl. Catal. A: Gen.* 326:121-129.
- [50] Wagner CD, Riggs WM, Davis RD, Moulder JF (1978). In *Handbook of X-ray Photoelectron Spectroscopy*. Muilenberg. G.E., Ed. Perkin-Elmer: Eden Preirrie, MN.
- [51] NIST X-ray Photoelectron Spectroscopy Database NIST Standard Reference Database 20, Version 3.5 (Web Version), National Institute of Standards and Technology, USA, 2007.
- [52] Liprandi DA, Cagnola EA, Paredes JF, Badano JM, Quiroga M E (2012) A High (Z)/(E) Ratio Obtained During the 3-Hexyne Hydrogenation with a Catalyst Based on a Rh(I) Complex Anchored on a Carbonaceous Support. *Catal. Lett.* 142: 231-237.
- [53] L'Argentièrre P, Quiroga M, Liprandi D, Cagnola E., Román Martínez MC, Díaz Auñón JA, Salinas Martínez de Lecea C. (2003) Activated carbon heterogenized [PdCl₂(NH₂(CH₂)₁₂CH₃)₂] for the selective hydrogenation of 1-heptyne. *Catal. Lett.* 87: 97 - 101.
- [54] Liprandi DA, Cagnola E A, Quiroga M E, L'Argentièrre PC (2009) Influence of the Reaction Temperature on the 3-Hexyne Semi-Hydrogenation Catalyzed by a Palladium(II) Complex. *Catal. Lett.* 128: 423-433
- [55] Cotton FA, Wilkinson G (1988) *Advanced Inorganic Chemistry*, fifth ed, John Wiley and Sons, New York, pp 901-902.

- [56] Purcell KF, Kotz JC (1977) *Inorganic Chemistry*, Holt-Saunders International Editions: Philadelphia, pp 543-549.
- [57] Papp A, Molnár A, Mastalir A (2005) Catalytic investigation of Pd particles supported on MCM-41 for the selective hydrogenations of terminal and internal alkynes. *Appl. Catal. A: Gen.* 289: 256-266.

IntechOpen

IntechOpen